Robust Nonlinear Control for a Piezoelectric Actuator in a Robotic Hand Using Only Position Measurements

Gerardo Flores, *Member, IEEE*, and Micky Rakotondrabe, *Member, IEEE*

***Abstract*—A robust nonlinear control based only on position measurements to compensate for the strong hysteresis nonlinearity in a piezoelectrically actuated robotic hand is proposed. Based on a high-gain observer to estimate the hysteresis response and nonlinear control law, locally exponential stable results are obtained. The observer and controller are arranged to conform to an output-feedback scheme, which is simple to implement and does not require additional computation as soon as the model parameters are identified and known. The proposed control technique is valuable for hysteresis that is modeled with the classical Bouc-Wen model. The results provide a closed-loop system that is robust under external disturbances in all the system states. Simulations show the effectiveness of the approach.**

***Index Terms*—Bouc-Wen hysteresis, Hammerstein model, output feedback control, perturbed system, piezoelectric actuator, robust nonlinear control.**

I. Introduction

PIEZOELECTRIC actuators are widely employed in systems that require both high resolution and high bandwidth. They can achieve positioning resolution down to tens of nanometers, and a first resonance frequency exceeding the kilohertz [1]. In counterpart, piezoelectric actuators and systems are typified by hysteresis and creep nonlinearities that drastically affect the final positioning precision if not compensated for. These nonlinearities are much stronger when the piezoelectric actuator is a ceramics material. In the context of a parallel robot (see Fig. 1-a) for precise manipulation of a deformable object, we develop a robotic hand of which the fingers are three piezoelectric actuators placed at its extremity (Fig. 1-b). When a voltage u is applied to each of the three actuators, they elongate along their respective y axis (Fig. 1-c), resulting in a closening of the hand. The actuators are based on PZT (lead zirconate titanate) ceramics piezoelectric materials. Hence, they exhibit strong hysteresis nonlinearity, creep nonlinearity, and badly damped vibrations response in their behavior. Whilst the creep nonlinearity, which occurs at shallow frequency excitation, and the vibrations were successfully compensated for in our previous works [2], [3], the hysteresis requires more attention as it can affect the closed-loop stability if the controller is not appropriately designed. Therefore, this letter is focused on the design of a control law that guarantees stability for the piezoelectric actuator, which exhibits strong hysteresis nonlinearity.

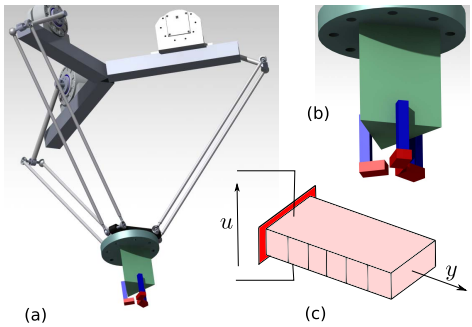

Fig. 1. (a): parallel robotic platform. (b): robotic hand with three fingers. (c): one piezoelectric actuator as a finger.

A. Related Work

The literature presents two principal architectures for controlling piezoelectric systems with hysteresis: feedforward and feedback. The motivation to design a feedforward control is mainly due to the lack of appropriate sensors when the piezoelectric actuators are devoted to limited space or miniaturized systems. The principle consists of modeling very precisely the hysteresis and then putting in cascade with the real system the inverse of the model as a nonlinear compensator. If the model is not invertible, an approximate operator of the inverse model is used. Three classes of models were principally used for that: the Bouc-Wen class [4], the Prandtl-Ishlinskii class [5], [6] and the Preisach class [7]. Whilst feedforward

Manuscript received March 4, 2021; revised May 11, 2021; accepted May 28, 2021. Date of publication June 7, 2021; date of current version June 30, 2021. Recommended by Senior Editor G. Cherubini. *(Corresponding author: Gerardo Flores.)*

Gerardo Flores is with the Laboratorio de Percepción y Robótica, Center for Research in Optics, León 37150, Mexico (e-mail: gflores@cio.mx).

Micky Rakotondrabe is with the Laboratoire Génie de Production, National School of Engineering in Tarbes (ENIT—INPT), University of Toulouse, 65000 Tarbes, France (e-mail: mrakoton@enit.fr).

Digital Object Identifier 10.1109/LCSYS.2021.3087102

control is not expensive (no sensor required), its main drawback is the lack of robustness versus external disturbances and model uncertainties. In feedback architecture, the literature includes i) model-based control design where a nonlinear hysteresis model is exploited, and ii) control design with an approximation of the hysteresis. The latter case is the most used as it permits to employ of standard linear control techniques. However, the approach does not formally permit to guarantee the stability or the prescribed performances of the closed-loop when the hysteresis is stronger. In model-based control design, very few models have been exploited. In [8], a Prandtl-Ishlinskii model was exploited to predict the stability when a repetitive control was employed. In [9] and [10], the Bouc-Wen class of models was used to design adaptive controllers. In fact, the Bouc-Wen class of models, which is differential equations-based models, has a favorable structure to stability analysis and controller synthesis, contrary to the Prandtl-Ishlinskii class. Though, in the above works, [9] and [10], the controllers and the stability analysis were not performed based on all parameters of the models but of some of them only, which therefore does not permit ensure the robustness when the hysteresis amplitude changes entirely.

B. Contribution

This letter suggests designing a feedback controller based on the classical Bouc-Wen hysteresis model in a piezoelectrically actuated robotic hand with strong hysteresis. To this aim, an output feedback architecture that uses the only available position information complemented with a nonlinear observer is proposed to overcome the limitation of sensors. The proposed observer estimates both the actuator's dynamics and the hysteresis state; it is an explicit function of the Bouc-Wen model's parameters. The controller ensures position tracking and external disturbance rejection. Finally, we prove that the closed-loop system is locally exponentially stable.

C. Content

The remainder of this letter is as follows. Section II presents the system modeling and poses the problem. In Section III the nonlinear observer is given, and the proof of convergence is provided. The control algorithm based on an output-feedback scheme is presented in Section IV, where a virtual control h_d to stabilize part of the system is computed. Furthermore, the computation of the real control u is presented in the same section. Simulation results of the closed-loop system with and without external disturbances are given in Section V. Finally, conclusions and perspectives are discussed in Section VI.

II. Problem Setting

The considered piezoelectric actuator can be represented by a Hammerstein structure as depicted in Fig. 2, where u is the driving voltage, y is the output position, and v is an intermediary signal. In fact, the piezoelectric actuator is constituted of a transduction part and the mechanical structure or plant. The transduction part, which converts the electrical energy into mechanical one, is known to contain hysteresis nonlinearity, while the mechanical structure exploits the mechanical energy

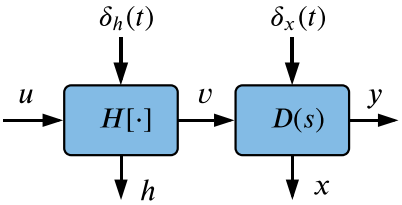

Fig. 2. Hammerstein model for the piezoelectric actuator under disturbances (δ_h, δ_x).

to create the movement. Consequently, the overall model of a piezoelectric actuator comprises a hysteresis submodel followed by a linear dynamics submodel, which is a Hammerstein structure [11].

The hysteresis is represented by the operator $H[\cdot]$ whilst the linear dynamics, by a transfer function $D(s)$. To account for possible external perturbation (for instance, the manipulated object's reaction), we introduce δ_h and δ_x. $(\delta_h(t), \delta_x(t))$ are assumed to be unknown and uncorrelated signals and unmodeled terms. Considering the classical Bouc-Wen hysteresis model [4] for $H[\cdot]$ and putting in state-space representation the dynamics, the system model is:

$$\Sigma: \begin{cases} \dot{h} = A_{bw}\dot{u} - B_{bw}|\dot{u}|h - G_{bw}\dot{u}|h| + \delta_h(t) & \text{(1a)} \\ \dot{x} = Ax + B\underbrace{(d_p u - h)}_{v} + \delta_x(t) & \text{(1b)} \\ y = Cx & \text{(1c)} \end{cases}$$

where (1a) is the hysteresis state equation with h being the internal state, and (1b) is the linear dynamics $D(s)$ with x the state, and (1c) the output. Notice that the input of subsystem (1b) is also written as $v = d_p u - h$ in the classical Bouc-Wen model [4]. The hysteresis model parameters are d_p, which indicates the initial slope, A_{bw} which controls the hysteresis amplitude, and B_{bw} and G_{bw} which control its shape. Moreover, the parameters of the dynamics are A, B, and C. All the parameters, including those of the dynamics, are scalar for the studied piezoelectric actuator, as we have one state element in x, single input u and single output y.

Without loss of generality consider $C = 1$ in (1c). The problem is as follows.

Problem 1: Given system Σ with available variables (u, y), the problem is to stabilize the state $y(t)$ to a desired trajectory $y_d(t)$.

Since only (u, y) are available, we propose an output-feedback control structure. Therefore, an observer to estimate the states (x, h) to control the system is suggested next.

III. Observer

Several important efforts have been conducted by researchers in the subject of nonlinear observers [12], [13], [14], [15], among others. These works motivate us to propose a simple but practical nonlinear observer, a fundamental part of our control introduced in the following section. Let us begin by studying the observability of system Σ.

Lemma 1: Assuming that $B \neq 0$, the system Σ is observable.

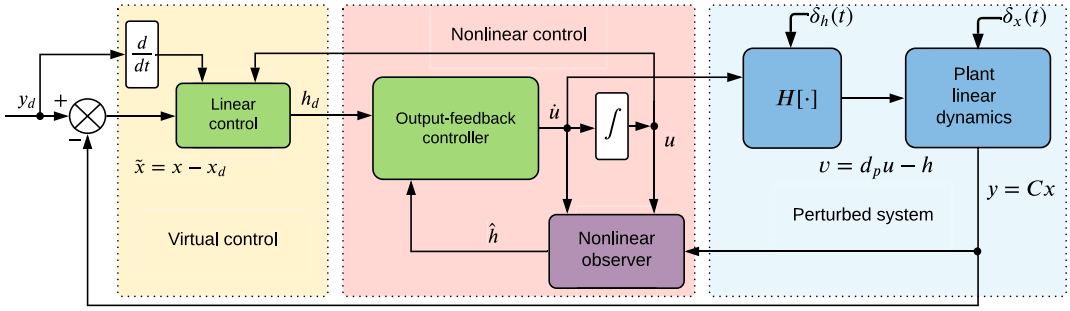

Fig. 3. Block diagram proposed showing the controls and the piezoelectrically actuated robotic hand system under disturbances.

Proof: Notice that we can arrange system Σ as follows

$$\begin{aligned} \dot{z} &= \Gamma z + g(z, \dot{u}) + \delta(t) \\ y &= \bar{C} z \end{aligned} \tag{2}$$

where $\bar{C} = [1,\ 0]$, $z = [z_1,\ z_2]^\intercal = [x,\ h]^\intercal$, $g(z, \dot{u}) = [Az_1 + Bd_p u,\ f(h, \dot{u})]^\intercal$, $\delta(t) = [\delta_x, \delta_h]^\intercal$, and $\Gamma = \begin{pmatrix} 0 & -B \\ 0 & 0 \end{pmatrix}$. Then, since $\operatorname{rank} \mathcal{O} = 2$, where $\mathcal{O} = [\bar{C},\ \bar{C}\Gamma]^\intercal$ is the observability matrix, the system Σ is observable as long as $B \neq 0$. ■

For the design of an observer of system (2) consider the following assumptions.

Assumption 1: The control input $u(t)$ and its time-derivative $\dot{u}(t)$ are bounded.

Assumption 2: The disturbance vector $\delta(t) = [\delta_x, \delta_h]^\intercal$ in (2) is bounded by $\|\delta\| \leq \varrho\|\epsilon\|$, where $\epsilon = \hat{z} - z$ is the observation error, and $\varrho \in \mathbb{R}^+$.

The observer is given in the following proposition.

Proposition 1: Consider Assumptions 1 and 2 and let S the solution of the following Lyapunov-like equation

$$\theta S + \Gamma^\intercal S + S\Gamma - C^\intercal C = 0, \tag{3}$$

then, the observer

$$\dot{\hat{z}} = \Gamma \hat{z} + g(\hat{z}, \dot{u}) - S^{-1} C^\intercal (\hat{z}_1 - z_1) \tag{4}$$

globally exponentially stabilizes the origin $\epsilon = \hat{z} - z$.

Proof: The solution of (3) is given by $S = \begin{pmatrix} \frac{1}{\theta} & \frac{B}{\theta^2} \\ \frac{B}{\theta^2} & \frac{2B^2}{\theta^3} \end{pmatrix}$ which is a symmetric positive definite matrix for $\theta \in \mathbb{R}^+$ [13], [16]. Now let us define the error $\epsilon = \hat{z} - z$, with time-derivative

$$\dot{\epsilon} = \left(\Gamma - S^{-1} C^\intercal C\right)\epsilon + g(\hat{z}, \dot{u}) - g(z, \dot{u}) - \delta(t). \tag{5}$$

Consider the following candidate Lyapunov function $W = \epsilon^\intercal S \epsilon$ whose time-derivative along the solutions of system (2) and observer (4) is given by

$$\dot{W} = 2\epsilon^\intercal \left(S\Gamma - C^\intercal C\right)\epsilon + 2\epsilon^\intercal S\left(g(\hat{z}, \dot{u}) - g(z, \dot{u}) - \delta(t)\right). \tag{6}$$

From (3) and Assumptions 1 and 2, it follows that

$$\begin{aligned} \dot{W} &\leq -2\epsilon^\intercal \left(\theta S + \Gamma^\intercal S\right)\epsilon + 2\|\epsilon\|\|S\|\left\|g(\hat{z}, \dot{u}) - g(z, \dot{u})\right\| \\ &\quad + 2\|\epsilon\|\|S\|\|\delta\| \\ &\leq -\theta \epsilon^\intercal S \epsilon + 2 l_g \|\epsilon\|^2 \|S\| + 2\varrho\|\epsilon\|^2\|S\|, \end{aligned} \tag{7}$$

since $S\Gamma - C^\intercal C = -\theta S - \Gamma^\intercal S$ is negative definite by (3), and l_g is the largest Lipschitz constant of $g(z, \dot{u})$ it follows that $\dot{W} \leq -(\theta - 2l_g - 2\varrho)W$. From this, and since W is radially unbounded, the equilibrium point ϵ is globally exponentially stable as long as $\theta > 2(l_g + \varrho)$; hence the proof is complete. ■

Remark 1: A large θ can significantly reduce the unknown disturbance vector's effect in the estimation problem. However, a large θ may lead to *peaking phenomenon* in transient response. This peaking phenomenon in practice can be reduced using saturations in the observer, as suggested by Atassi and Khalil [14], Flores *et al.* [17].

IV. Control

To control subsystem (1b) with output (1c), we use the signal h for feedback control, since in that system, h represents an exogenous signal. The reference for h control will be denoted by h_d. Such a value will be the desired state for subsystem (1a) with controller input $\dot{u}$. From the separation principle [14], we design separately the control and the observer. A scheme of the proposed control approach is depicted in Fig. 3.

A. Control for the Linear Dynamics Part (1b)-(1c)

The virtual control input for subsystem (1b) with output (1c) will be h_d. We take into account the following assumption.

Assumption 3: The system individual disturbances are bounded: $|\delta_x| \leq \varrho_1|\tilde{x}|$, and $|\delta_h| \leq \varrho_2|e|$, where $\tilde{x} = x - x_d$, and $e = h - h_d$.

The first result is summarized next.

Proposition 2: Consider the system (1b) with output (1c). Then, the virtual control

$$h_d = \frac{1}{B}\left([A + \kappa_1]\tilde{x} + Ax_d - \dot{x}_d + Bd_p u\right) \tag{8}$$

globally asymptotically stabilizes $\{\tilde{x} = 0\}$, where $\tilde{x} = x - x_d$, if $\kappa_1 > \varrho_1$, and $|\delta_x| \leq \varrho_1|\tilde{x}|$ holds (first part of Assumption 3).

Proof: Let us propose the following candidate Lyapunov function $V_{\tilde{x}} = \frac{1}{2}\tilde{x}^2$, whose time-derivative along the solutions of (1b) is

$$\dot{V}_{\tilde{x}} = \tilde{x}\dot{\tilde{x}} = \tilde{x}\left(A[\tilde{x} + x_d] + Bd_p u - Bh + \delta_x(t) - \dot{x}_d\right). \tag{9}$$

Substituting the control (8) and assuming that $h \to h_d$ in system (1a), after Assumptions 1 and 3, it follows that

$$\dot{V}_{\tilde{x}} = \tilde{x}\big(A\tilde{x} + Ax_d + Bd_p u + \delta_x(t) - B\left(\frac{1}{B}\big([A+\kappa_1]\tilde{x} + Ax_d - \dot{x}_d + Bd_p u\big)\right) - \dot{x}_d\Big) \leq -\kappa_1\tilde{x}^2 + \varrho_1|\tilde{x}|^2 \leq -(\kappa_1 - \varrho_1)\tilde{x}^2 \quad (10)$$

thus, the closed-loop system (1b)-(1c)-(8) is globally exponentially stable since $B \neq 0$, $\kappa_1 > \varrho_1$, and u is bounded by assumption. ■

B. Control for Sub-System (1a)

Once we have obtained the desired value $h_d(t)$ for subsystem (1b) with output (1c), we continue to solve the tracking problem for subsystem (1a). For it, let us consider that the first time-derivative of the control input u, i.e., $\dot{u}$, is a control variable for (1a).

Assumption 4: The desired signal h_d in (8) and its time derivative $\dot{h}_d$ are bounded by

$$|h_d| \leq c_1, \;\; |\dot{h}_d| \leq c_2|e|, \quad (11)$$

with $c_1, c_2 \in \mathbb{R}^+$, where $e = h - h_d$.

Proposition 3: Consider Assumption 4 and inequality $|\delta_h| \leq \varrho_2|e|$ (second part of Assumption 3), then the control

$$\dot{u} = \frac{1}{A_{bw}}\Big(-k_1 \operatorname{sgn}(e)\sqrt{|e|} - k_2 e\Big) \quad (12)$$

locally exponentially stabilizes subsystem (1a).

Proof: Let us define the error $e = h - h_d$ with dynamics

$$\dot{e} = \dot{u}(A_{bw} - G_{bw}|e + h_d|) - B_{bw}|\dot{u}|(e + h_d) + \delta_h(t) - \dot{h}_d \quad (13)$$

Let us consider the candidate Lyapunov function $V_c = |e|$. The time derivative of V_c along the trajectories of (13) is

$$\dot{V}_c = \operatorname{sgn}(e)\Big(\dot{u}(A_{bw} - G_{bw}|e + h_d|) - B_{bw}|\dot{u}|(e + h_d) + \delta_h(t) - \dot{h}_d\Big) \leq -k_1\sqrt{|e|} - k_2|e| + |G_{bw}||\dot{u}||e + h_d| - B_{bw}|\dot{u}||e| + |B_{bw}||\dot{u}||h_d| + |\delta_h| + |\dot{h}_d|. \quad (14)$$

Taking into account both the second part of the Assumption 3 and the Assumption 4, it follows that

$$\dot{V}_c \leq -k_1\sqrt{|e|} - k_2|e| + (|G_{bw}| - B_{bw})|\dot{u}||e| + c_1(|G_{bw}| + |B_{bw}|)|\dot{u}| + \varrho_2|e| + c_2|e|. \quad (15)$$

When $B_{bw} > 0$, the term $-B_{bw}|\dot{u}||e|$ contributes to the desired negative definiteness of $\dot{V}_c$. Then, to cover any value of B_{bw} in the stability analysis, we also included the scenario when $B_{bw} < 0$, thus we consider the term $(|G_{bw}| + |B_{bw}|)$ in the following[1]:

$$\dot{V}_c \leq -k_1\sqrt{|e|} - k_2|e| + \frac{\alpha}{|A_{bw}|}(|G_{bw}| + |B_{bw}|)\sqrt{|e|}|e| + \frac{c_1\alpha}{|A_{bw}|}(|G_{bw}| + |B_{bw}|)\sqrt{|e|} + \varrho_2|e| + c_2|e|, \quad (16)$$

[1]Notice that G_{bw} can take any positive or negative value, the stability analysis considers both cases.

where we have used the fact that $|\dot{u}| \leq \frac{1}{|A_{bw}|}(k_1\sqrt{|e|} + k_2|e|)$ together with inequality

$$k_1\sqrt{|e|} + k_2|e| \leq \alpha\sqrt{|e|} \quad (17)$$

where α is a sufficiently large positive number. The last expression is valid as long as $|e| \leq (\frac{\alpha - k_1}{k_2})^2$ holds. Then

$$\dot{V}_c \leq -\left(k_1 - \frac{c_1\alpha}{|A_{bw}|}(|G_{bw}| + |B_{bw}|)\right)\sqrt{|e|} - (k_2 - \varrho_2 - c_2)|e| + \frac{\alpha}{|A_{bw}|}(|G_{bw}| + |B_{bw}|)\sqrt{|e|}|e| \leq -\sigma\sqrt{|e|} - \beta|e| + \rho\sqrt{|e|}|e| \quad (18)$$

where

$$\sigma = k_1 - c_1\rho, \;\; \beta = k_2 - \varrho_2 - c_2, \;\; \rho = \frac{\alpha}{|A_{bw}|}(|G_{bw}| + |B_{bw}|). \quad (19)$$

are tuned to be positive real numbers with the aim of $\dot{V}_c$ in (18) be negative definite when:

$$|e| \leq \min\left\{\left(\frac{\alpha - k_1}{k_2}\right)^2, \frac{\beta\sqrt{4\sigma\rho + \beta^2} + 2\sigma\rho + \beta^2}{2\rho^2}\right\} \quad (20)$$

holds, and hence the equilibrium point $\{e = 0\}$, where $e = h - h_d$, is locally exponentially stable. ■

Remark 2: The control (12) can be solved by numerical integration with the aim of finding u.

C. Output Feedback Control

So far, we have designed in a separate way the observer and the controller. The observer's main goal was to get an estimate $\hat{h}$ required for feedback in the control algorithm (12). Therefore, the pair observer-controller as an *output-feedback control* can be applied. Such output-feedback control is the previously defined controller (12) combined with the output of the observer (4). Hence, this is given as follows:

$$\dot{u} = \frac{1}{A_{bw}}\Big(-k_1 \operatorname{sgn}(\hat{h} - h_d)\sqrt{|\hat{h} - h_d|} - k_2(\hat{h} - h_d)\Big). \quad (21)$$

To prove that the equilibrium point $(\epsilon, \tilde{x}, e)$ of the system Σ together with (4)-(8)-(21) is asymptotically stable, we use the separation-principle results established in [14], [18], and [19]. In particular, since system Σ is in cascade form (see (2)), we apply [18, Th. 3] with Lyapunov function $V = V_{\tilde{x}} + V_c$ and output-feedback control (21).

Remark 3: The virtual control (8) remains the same for with or without observer since it depends on the available signal $y = x$.

Remark 4: The output-feedback control does not require to accomplish any restriction of the Bouc-Wen model parameters A_{bw}, B_{bw}, and G_{bw}. In other words, we demonstrated that for any values of such parameters, the controller ensures stability.

V. Simulation Results

In the sequel, we will not display the units of signals and parameters. They are: μm for y, y_d, x and h; and Volt for u. The units of the parameters A_{bw}, B_{bw}, G_{bw} and d_p are automatically in accordance with these. Their values for the simulation are

TABLE I
SET OF PARAMETERS USED IN THE SIMULATION

Parameters set	d_p $(\mu m/V)$	A_{bw}	B_{bw}	G_{bw}
No. 1	1.0773	0.40648	0.00833	0.00833
No. 2	1.6	0.9	0.008	0
No. 3	10	0.4297	0.03438	-0.002865
No. 4	0.2	0.2	-0.002	0.04

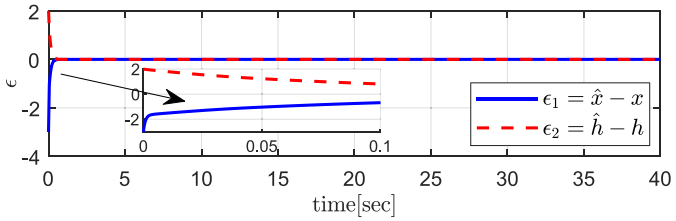

Fig. 4. The convergence of the observer error ϵ to zero.

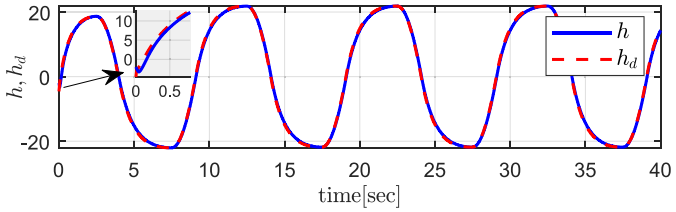

Fig. 5. Hysteresis control. The convergence of the system state h to h_d thanks to control (21).

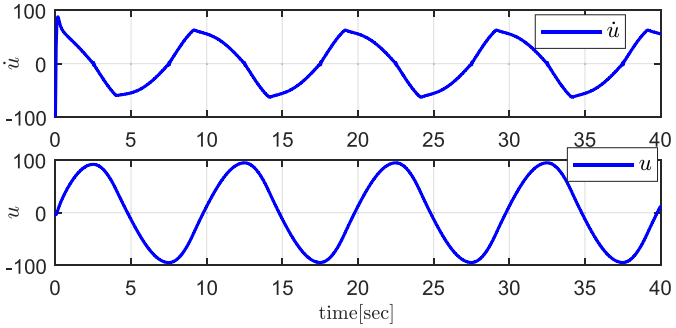

Fig. 6. The control u, in (21), and its first-time derivative $\dot{u}$.

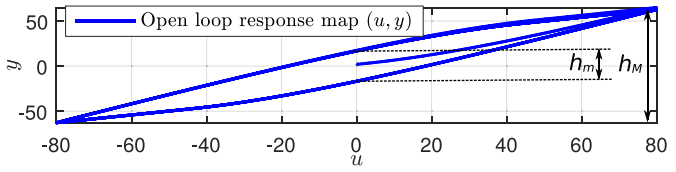

(a) Open-loop system response.

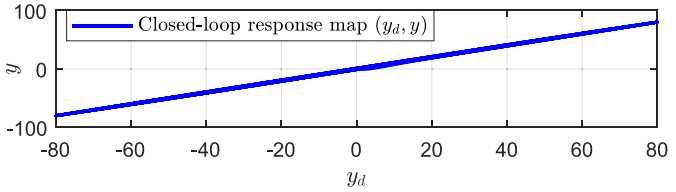

(b) Closed-loop system response.

Fig. 7. Input-output responses: (a) (u, y) map for the open-loop system, and (b) (y_d, y) map for the closed-loop system.

chosen considering the set of values as shown in Table I; in all the cases $C = [1,\ 0]$ (and hence $y_d = x_d$ hereafter). The control parameters are $k_1 = 20$, $k_2 = 15$, $\kappa_1 = 500$. The observer parameter is $\theta = 100$. The reference signal is chosen as $x_d = 80 \sin \frac{2\pi}{10} t$ where the frequency is 0.1 Hz. The linear system parameter is $A = -\frac{1}{\tau}$, and $b = \frac{1}{\tau}$ where $\tau = 0.001s$. The initial conditions for the observer are zero, and for the system is $[x, h]^\intercal = [3, -2]^\intercal$. The simulation is performed in MATLAB Simulink using a fixed-step of $0.0001s$, and the ode5 Dormand-Price solver.

Let us consider the parameter set No. 1 in Tab. I for the following simulation. The simulation corresponds to the system Σ with observer (4), and controls (8), (21). We start by assuming that the system are free of any disturbance. The error observer $\epsilon = \hat{z} - z$ corresponding to the dynamics of (5) is depicted in Fig. 4. The convergence rate is defined by the magnitude of the parameter θ in S.

The convergence of the system state x to x_d is shown in the left upper corner of Fig. 8. Notice how the hysteresis effect does not affect the convergence. Besides, the virtual control h_d is depicted in Fig. 5 where the effect of control (12) makes h converges to h_d.

The real control input u and its first-time derivative are depicted in Fig. 6.

For comparison purposes, let us consider the open-loop response, i.e., the system Σ only, without the controller nor the observer. Then, let us apply a sinusoidal voltage u of frequency $0.1Hz$ and a voltage such that the output reaches $80\mu m$. The resulting curve in the (u, y) map is shown in Fig. 7(a), which reveals the actuator's strong hysteresis property when without control. Indeed, the hysteresis amplitude is of $h_{amp} = \frac{h_m}{h_M} \approx \frac{35}{120} = 25\%$ which is strong. Let us plot the input-output map using the proposed controller combined with the observer, i.e., the (y_d, y)-map, when applying a sinusoidal reference y_d of the same frequency and amplitude $80\mu m$. Fig. 7(b) shows the results where the hysteresis is completely removed.

To highlight that our control is independent of the variability in the parameters of the hysteresis model, we simulate the closed-loop system for the rest of the parameter set in Tab. I. The results are shown in Fig. 8, where it is clear that the control achieved good performance for all the parameters set.

To numerically study the robustness behavior of our approach, we conduct simulation under external disturbances for the parameter set No. 1 in Tab. I. The disturbances are chosen as $\delta_x = 30\mu m$, and $\delta_h = 25 \sin(t)\mu m$. The system response is depicted in Fig. 9 for the open-loop and closed-loop cases. Notice how disturbances affect the system response in the closed-loop case with an approximately 4 μm in the curve's low peak, around $t = 7.5$s. Adjusting the control and observer gains can reduce the error. However, this displacement is small, considering that the disturbances are relatively high with respect to the desired trajectory magnitude. For instance, δ_x is 37.5% the value of the desired magnitude which is equal to 80 μm. If we compare Fig. 9(b) to the response

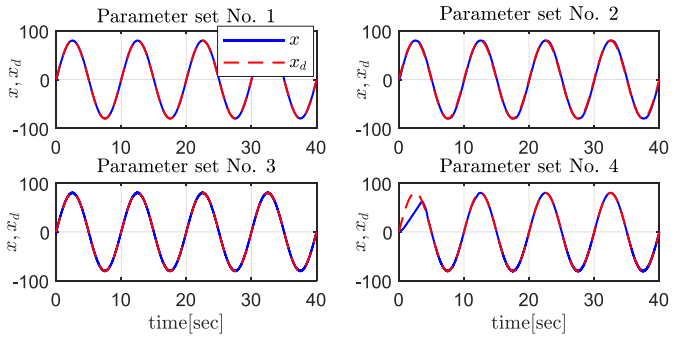

Fig. 8. Input-output response with set of parameters corresponding to Table I.

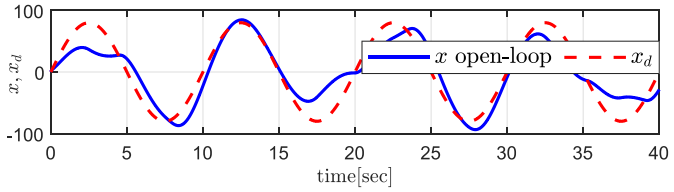

(a) Open-loop system response.

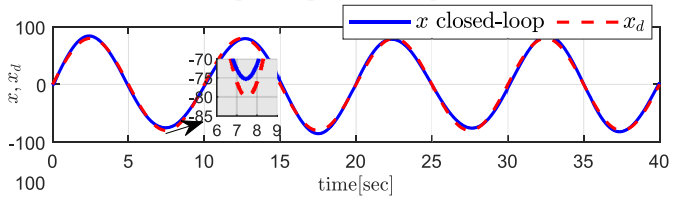

(b) Closed-loop system response.

Fig. 9. Input-output response for the open-loop system (a) and the closed-loop system (b) under the effect of disturbances.

depicted in the left upper corner of Fig. 8 where no disturbances are presented, the effect can be considered minimal. On the other hand, the open-loop system response results are highly disturbed, as shown in Fig. 9(a).

VI. Conclusion

A robust feedback control algorithm to stabilize a piezoelectrically actuated robotic hand with strong hysteresis was proposed in this letter. The actuator model was given as a Hammerstein structure based on the classical Bouc-Wen hysteresis model and linear dynamics. Due to the lack of measurement sensors, we only use available position measurements in the control algorithm. Consequently, we design a nonlinear observer to estimate both the dynamics' internal state and the hysteresis nonlinearity state. Both the observer's convergence and the closed-loop local exponential stability were demonstrated. Besides, the controller was designed to reject external disturbances. Several simulations were carried out and demonstrated the efficiency of the introduced observer and control approach.

Experimental tests on a real piezoelectric actuator-based benchmark are expected as perspectives to validate the proposed strategy in this letter.

References

[1] S. Devasia, E. Eleftheriou, and S. O. R. Moheimani, "A survey of control issues in nanopositioning," *IEEE Trans. Control Syst. Technol.*, vol. 15, no. 5, pp. 802–823, Sep. 2007.

[2] M. Rakotondrabe, "Modeling and compensation of multivariable creep in multi-DOF piezoelectric actuators," in *Proc. IEEE Int. Conf. Robot. Autom.*, May 2012, pp. 4577–4581.

[3] Y. Al Hamidi and M. Rakotondrabe, "Multi-mode vibration suppression in a multi-DOF piezoelectric tube actuator by extending the zero placement input shaping technique," *Actuators*, vol. 48, no. 5, p. 13, Mar. 2016.

[4] M. Rakotondrabe, "Bouc-Wen modeling and inverse multiplicative structure to compensate hysteresis nonlinearity in piezoelectric actuators," *IEEE Trans. Autom. Sci. Eng.*, vol. 8, no. 2, pp. 428–431, Apr. 2011.

[5] M. Rakotondrabe, "Multivariable classical prandtl-ishlinskii hysteresis modeling and compensation and sensorless control of a nonlinear 2-DOF piezoactuator," *Nonlinear Dyn.*, vol. 89, pp. 481–499, Mar. 2017.

[6] M. Al Janaideh and P. Krejčí, "Inverse rate-dependent Prandtl–Ishlinskii model for feedforward compensation of hysteresis in a piezomicropositioning actuator," *IEEE/ASME Trans. Mechatronics*, vol. 18, no. 5, pp. 1498–1507, Oct. 2013.

[7] K. K. Leang, Q. Zou, and S. Devasia, "Feedforward control of piezoactuators in atomic force microscope systems," *IEEE Control Syst. Mag.*, vol. 29, no. 1, pp. 70–82, Feb. 2009.

[8] Y. Shan and K. K. Leang, "Accounting for hysteresis in repetitive control design: Nanopositioning example," *Automatica*, vol. 48, no. 8, pp. 1751–1758, 2012.

[9] J.-A. Escareno, M. Rakotondrabe, and D. Habineza, "Backstepping-based robust-adaptive control of a nonlinear 2-DOF piezoactuator," *Control Eng. Pract.*, vol. 41, pp. 51–71, Aug. 2015.

[10] M. H. M. Ramli, T. V. Minh, and X. Chen, "Pseudoextended Bouc–Wen model and adaptive control design with applications to smart actuators," *IEEE Trans. Control Syst. Technol.*, vol. 27, no. 5, pp. 2100–2109, Sep. 2019.

[11] M. Rakotondrabe, *Smart Materials-Based Actuators at the Micro/Nano-Scale: Characterization, Control and Applications*. New York, NY, USA: Springer-Verlag, Mar. 2013.

[12] G. Besançon, *Nonlinear Observers and Applications*, 1st ed. Heidelberg, Germany: Springer-Verlag, 2007.

[13] K. Busawon, M. Farza, and H. Hammouri, "A simple observer for a class of nonlinear systems," *Appl. Math. Lett.*, vol. 11, no. 3, pp. 27–31, May 1998.

[14] A. N. Atassi and H. Khalil, "A separation principle for the control of a class of nonlinear systems," *IEEE Trans. Autom. Control*, vol. 46, no. 5, pp. 742–746, May 2001.

[15] G. Besançon, G. Bornard, and H. Hammouri, "Observer synthesis for a class of nonlinear control systems," *Eur. J. Control*, vol. 2, no. 3, pp. 176–192, 1996.

[16] J. P. Gauthier, H. Hammouri, and S. Othman, "A simple observer for nonlinear systems applications to bioreactors," *IEEE Trans. Autom. Control*, vol. 37, no. 6, pp. 875–880, Jun. 1992.

[17] G. Flores, V. González-Huitron, and A. Rodríguez-Mata, "Output feedback control for a quadrotor aircraft using an adaptive high gain observer," *Int. J. Control Autom. Syst.*, vol. 18, pp. 1474–1486, Feb. 2020.

[18] A. Loría and J. de León Morales, "On persistently exciting observers and a non-linear separation principle: Application to the stabilization of a generator," *Int. J. Control*, vol. 76, no. 6, pp. 607–617, 2003.

[19] G. Flores and M. Rakotondrabe, "Output feedback control for a nonlinear optical interferometry system," *IEEE Control Syst. Lett.*, vol. 5, no. 6, pp. 1880–1885, Dec. 2021.